Quantum Non-Gaussianity of Multiphonon States of a Single Atom

L. Podhora,[1] L. Lachman,[1] T. Pham,[2] A. Lešundák,[2] O. Číp,[2] L. Slodička,[1,*] and R. Filip[1,†]
[1]Department of Optics, Palacký University, 17. listopadu 12, 77146 Olomouc, Czech Republic
[2]Institute of Scientific Instruments of the Czech Academy of Sciences, Královopolská 147, 612 64 Brno, Czech Republic

(Received 18 November 2021; revised 22 March 2022; accepted 25 May 2022; published 28 June 2022)

Quantum non-Gaussian mechanical states are already required in a range of applications. The discrete building blocks of such states are the energy eigenstates—Fock states. Despite progress in their preparation, the remaining imperfections can still invisibly cause loss of the aspects critical for their applications. We derive and apply the most challenging hierarchy of quantum non-Gaussian criteria on the characterization of single trapped-ion oscillator mechanical Fock states with up to 10 phonons. We analyze the depth of these quantum non-Gaussian features under intrinsic mechanical heating and predict their requirement for reaching quantum advantage in the sensing of a mechanical force.

DOI: 10.1103/PhysRevLett.129.013602

Introduction.—Long-term progress in nonlinear control of quantum mechanical states allows the deterministic generation of discrete quanta of energy embedded in a single motional mode [1–10]. They find direct application in quantum sensing [11,12]. This effort has opened many ways to generate other quantum non-Gaussian (QNG) states broadly useful in quantum metrology [9,13,14] and quantum error correction [8,15–17]. QNG aspects have also appeared as a consequence of nonlinear dynamics on oscillator ground states as well as in the broadly discussed quantum engines [18,19] and recently, in quantum phase transitions [20]. Nonlinearity is always required in some form, since QNG properties can never arise from any mixture of Gaussian states produced by linearized dynamics [21,22]. In a continuous-variable representation, QNG states can exhibit a spectrum of negative values of a Wigner function [23]. For optical tests of QNG features belonging to Fock states with an unambiguous identification the possibilities beyond continuous-variable representations based on the Wigner function, hierarchies of criteria for photonic states have been derived and experimentally verified for up to three photons [24]. Recently, the Husimi function has also been used to define a stellar representation of QNG states [25]. They specifically accent the optical loss being the main limitation of propagating states of light. Note that the condition for genuine n-photon quantum non-Gaussianity introduced in [24] is equivalent to the stellar rank for Fock states [26].

Here, we experimentally demonstrate the most strict hierarchy of QNG criteria suitable for individual Fock states of mechanical systems, where mechanical heating is the critical limitation [27,28]. Therefore, Fock states of mechanical oscillators crucially deserve different criteria and analysis than states of light [24,26,29–33]. The nth order criteria applied to the phonon-number distribution can conclusively recognize that analyzed aspect of the oscillator state is not reachable by any mixture of $D(\alpha)S(r)\sum_{m<n-1} c_m|m\rangle$ with complex α, r and c_m, where $D(\alpha)$ and $S(r)$ are Gaussian displacement and squeezing operations applied to any superposition of Fock states up to n-1, and $\sum_m |c_m|^2 = 1$. It proves that a genuine Fock state $|n\rangle$ has been unambiguously generated and therefore the observed state can supply applications powered by its exclusive QNG aspects.

We verify this hierarchy [24,26] on states approaching Fock states for a motional mode of a trapped ion oscillator and provide a reference methodology for such an implementation together with analysis of the effect of the dominant deteriorating mechanism in mechanical systems—thermal heating. The resulting unprecedentedly high genuine QNG properties and the paramount possibility of their verification allow for an unambiguous analysis of the states powering applications requiring genuine QNG states of atomic motion for quantum enhanced sensing [9,12] or assist prospective directions of efficient qubit encoding and error correction [8,34], which require a clear and simple threshold-based experimental methodology. Although these works provided pioneering proof-of-principle demonstrations of sensing applications which provably require high probability of the Fock states [9,12], the feasibility, robustness, and experimental relationship to applications of the genuine QNG aspects could not be directly accessed or proven, despite their crucial role. We generate motional states of a single trapped ion with up to ten motional quanta to develop and test the methodology for the conclusive and unambiguous analysis of their genuine QNG properties [24,26]. We estimate their robustness to the heating relevant to mechanical systems and discover that the nth order criteria are more strict than basic quantum non-Gaussianity [35], negativity of the Wigner

function, and even observation of the largest negative annulus in the Wigner function corresponding to the Fock state $|n\rangle$ [36]. We confirm that QNG features correspond to the crucial and challenging resource powering quantum sensing of coherent displacement or recoil heating [12] by the estimation of sensing capability for the generated states and realize that genuine QNG features are indeed necessary for reaching high sensitivity.

Hierarchy of QNG criteria for mechanical Fock states.—Genuine n-phonon QNG defines phonon statistics that do not evolve from Gaussian processes modifying any superposition involving Fock states lower than $|n\rangle$. It determines a quantum aspect that these statistics share with the state $|n\rangle$, which cannot be achieved with all the lower Fock states. Formally, the genuine n-phonon QNG of pure states requires

$$|\psi_n\rangle \neq D(\alpha)S(r)\sum_{m=0}^{n-1} c_m|m\rangle, \tag{1}$$

where $S(r)=\exp[r(a^\dagger)^2-r^*a^2]$ and $D(\alpha)=\exp[\alpha^* a-\alpha a^\dagger]$ are the squeezing and displacement unitary operators, respectively, with a complex squeezing parameter r, complex displacement α, and a, $a^\dagger$ corresponding to ladder operators [24]. Both $D(\alpha)$ and $S(r)$ are Gaussian operations that correspond to linear transformations of the ladder operators and do not increase the non-Gaussianity of a state $\sum_{m=0}^{n-1} c_m|m\rangle$. An impure state possesses this quantum aspect when it does not correspond to any statistical mixture of the right side of (1). The most strict criterion uses a bosonic distribution $P_n = \langle n|\rho|n\rangle$ to recognize the genuine n-phonon QNG for the imperfect Fock state $|n\rangle$ when the probability p_n exceeds the threshold

$$\bar{p}_n = \max_{\alpha,r,c_0,\ldots,c_m} \left|\langle n|D(\alpha)S(r)\sum_{m=0}^{n-1} c_m|m\rangle\right|^2. \tag{2}$$

The linearity of the maximizing task for determining $\bar{p}_n$ guarantees that any mixture of rejected states cannot surpass $\bar{p}_n$. More details about the genuine QNG criteria suitable for mechanical systems can be found in the Supplemental Material, S1 [37]. We note that identical threshold values for p_n can be alternatively derived using the stellar representation of QNG states [26], which, in addition, provide analytical expressions for the thresholds for the considered Fock states.

A trapped-ion system with the possibility of unprecedented motional control and practically lossless readout is a suitable candidate for tests of the diverse QNG aspects of motion in a well-defined mode and with high experimental precision [1,3–9]. It allows for implementations with minimal added noise and promises prospects of accessing QNG features with feasible observations of the sensitive properties relevant for applications [8,9,12,50]. The experiment is implemented on the axial motional mode of a single $^{40}Ca^+$ ion held in a linear Paul trap. Figures 1(a) and 1(b) show a simplified scheme of the experimental arrangement and the experimental sequence [37]. The quantum motional states are generated by a transfer of the initial vacuum state to the state approaching the Fock state $|n\rangle$ by an iterative sequence of motional population raising operations corresponding to blue and red sideband π pulses on the $|g\rangle \sim 4S_{1/2}(m=-1/2) \leftrightarrow |e\rangle \sim 3D_{5/2}(m=-1/2)$ electronic transition with frequencies ω_b and ω_r, respectively [1,3,9]. The state preparation is followed by estimation of the phonon-number probabilities P_n using the precise analysis of Rabi oscillations on the first blue motional sideband [51].

Figure 1(c) analyzes the exhibition of genuine n-phonon quantum non-Gaussianity using idealized and measured Fock states (yellow data points). The simulations signify that the observability of the lowest QNG features (red points) characterized by $|\psi_n\rangle \neq D(\alpha)S(r)|0\rangle$ [35] in the presence of heating monotonically increases with n for ideal Fock states. On the contrary, the generation and observation of genuine QNG (blue points) for high Fock states inside the hierarchy (1) and (2) is challenging and its sensitivity to imperfections in the state preparation and detection increases with n. The ideal thermalization dynamics considered, corresponding to a Gaussian additive noise, can be broadly employed for an estimation of the QNG depth, analogous to how the damping was used for photonic implementations [31]. The thermal depth has been evaluated as the corresponding increase of the mean thermal energy $\bar{n}_{\mathrm{th}}$ for the same thermalization strength applied to the vacuum state. This allows for a platform-independent comparison of the genuine QNG states in mechanical systems. In turn, these measurements can also be employed for testing the quality of the mechanical system or for sensing the amount of inherent thermal noise. The thermal depth of the measured states is much smaller for the genuine QNG hierarchy (1) and (2), in contrast to the lowest QNG criteria [35] which are actually less demanding for higher Fock states. Still, the measured 10-phonon states conclusively proved the genuine QNG features. Although the absolute thermal depths shown as mean phonon numbers $\bar{n}_{\mathrm{th}}$ decrease both for the genuine QNG features (blue values) and for the lowest QNG criteria [35] (red values), their ratio increases to about an order of magnitude for $n = 10$. A further analysis can be found in the Supplemental Material, S3 and S4 [37].

Robustness of the genuine QNG.—In the vast majority of implementations of quantum mechanical oscillators with atoms and electromechanical systems, their manipulation and observation is accompanied by small heating [10,27,28]. The heating mechanisms relevant for the single-ion oscillator include photon recoil due to the spontaneous emission or interaction of the charged particle with the surrounding thermal trapping environment. On the

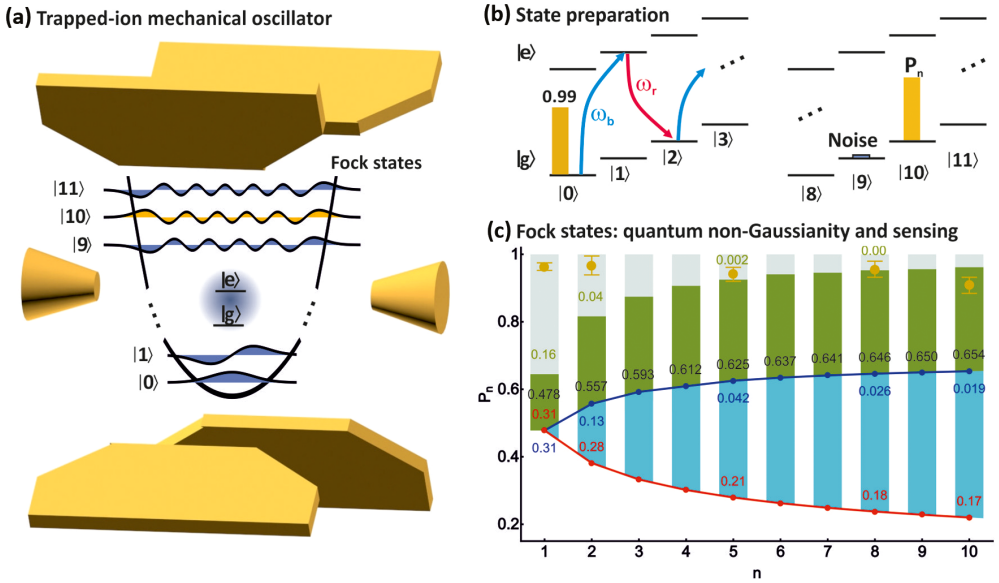

FIG. 1. (a) The mechanical oscillator corresponds to axial harmonic motion of a single $^{40}Ca^{+}$ ion localized in a linear Paul trap. The generation and analysis of states approaching idealized Fock states illustrated by their corresponding wave functions is implemented through interaction of the electronic ground $|g\rangle$ and metastable $|e\rangle$ states with the quantized harmonic motion on the first motional sidebands. (b) The sequence for preparation of genuine QNG states includes initialization to the electronic and motional ground state $|g, 0\rangle$ followed by deterministic transfer of the accumulated population to number states by repetitive coherent excitation of the blue and red sidebands depicted as blue and red arrows, respectively. The spectroscopic analysis of phonon number populations P_n around the target Fock state implements an unambiguous identification of the genuine QNG features. (c) Characterization of the Fock states of mechanical motion. The yellow points represent the measured populations P_n for the experimentally generated states. The thresholds for genuine n-phonon QNG are represented by blue points with the corresponding black numbers showing their numerical value [24,26]. The associated blue numbers quantify the thermal depth of genuine n-phonon QNG. Similarly, the red points identify thresholds for observation of basic QNG aspects [35] and the associated red numbers determine their thermal depth. The green bars depict the force estimation capability of a specific model of noisy Fock states, where the probability P_n exceeding the presented threshold values certifies a metrological advantage [12] against the previous ideal Fock state $|n-1\rangle$, while the corresponding numbers quantify the thermal depth of this advantage for the measured states.

short timescales relevant for the generation of target Fock states, the heating results in the error given predominantly by $P_{n-1} + P_{n+1}$. This assumption is confirmed by our observations of motional populations after the state preparation presented in the Supplemental Material, S2 [37]. The depth of QNG for states of mechanical systems can be naturally defined as the amount of heating necessary to reach the corresponding QNG boundary (1) and (2).

We study the QNG depth by the evaluation of the robustness of the generated QNG states to the mechanical heating induced by random photon recoils implemented by illuminating the ion with a short laser pulse on the $4S_{1/2} \leftrightarrow 4P_{1/2}$ transition. The heating rate has been set to $(115 \pm 2) \times 10^3$ ph/s on an ion prepared in the motional ground state. Figure 2 shows measurements of the relative depth scaled consistently to the mean added thermal energy when the same thermalization is applied to the vacuum state. The simulations employ a single-parameter photon recoil model, shown as red dashed curves. However, as the employed laser beam is set to optimize the Doppler cooling, the trajectories in the P_n, $P_{n-1} + P_{n+1}$ space are expected to deviate from this model for high initial Fock states or for very long thermalization times. A finite temperature reservoir characterized by two parameters [52] has to be included to plausibly explain the evolutions in these limits (green dashed curve). The observations confirm the predicted increased sensitivity of states with high order n of genuine QNG to heating, as can be seen by the gradually reduced scale of the effective mean thermal phonon number n_{th}. A detailed description of thermalization can be found in the Supplemental Material, S3 [37].

Force estimation capability.—A mechanical oscillator in a state approaching Fock state can be directly used for a phase-insensitive sensing of a weak force causing a tiny displacement α [12]. Let the oscillator be prepared in an initial state ρ and let $D(\alpha)$ denote the displacement operator characterizing the evolution that the force induces. The Fisher information for the estimation of the parameter $|\alpha|^2$ reads

$$F = \sum_{m=0}^{\infty} \frac{1}{P_m(|\alpha|^2)} \left[\frac{\mathrm{d}}{\mathrm{d}_{|\alpha|^2}} P_m(|\alpha|^2) \right]^2, \tag{3}$$

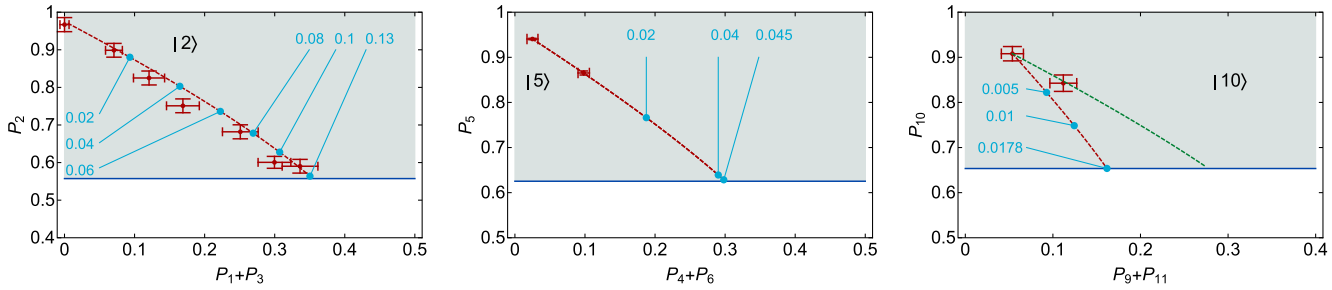

FIG. 2. Measurements of the QNG depth for states approaching Fock states $|2\rangle$, $|5\rangle$, and $|10\rangle$. Each graph shows the probability P_n and the overall probability $P_{n-1}+P_{n+1}$ relevant for the evaluation of the thermalization. The red points represent the measured states after several heating steps with an increasing length of the 397 nm laser pulse. The red dashed lines correspond to the theoretical model of ion heating by random photon recoils, with blue points giving a scale of the applied thermalization using an equivalent mean thermal phonon number $\bar{n}_{\mathrm{th}}$ when applied to the vacuum state. The green dashed line in a graph for state approaching $|10\rangle$ shows the simulated trajectory above the Doppler cooling limit and horizontal blue lines depict thresholds of the nth order genuine QNG [24,26] given by (1) and (2). For $n=2$ and 5 the green dashed lines coincide with the red dashed one.

where $P_n(|\alpha|^2)=\langle n|D(|\alpha|)\rho D^{\dagger}(|\alpha|)|n\rangle$ is the phonon-number distribution on which the sensing is performed. We evaluate the σ saturating the Cramér-Rao bound for the realized states. The metrological advantage R_ρ can be quantified according to

$$R_\rho(|\alpha|^2)=\frac{\sigma}{\sigma_0}, \tag{4}$$

where σ_0 stands for the standard deviation of the measurement for the mechanical probe prepared in the motional ground state. For ideal Fock states, (4) approaches

$$R_{|n\rangle}(|\alpha|^2)=\frac{1}{\sqrt{2n+1}}, \tag{5}$$

which is independent of the estimated $|\alpha|^2$. The full derivation can be found in the Supplemental Material, S5 [37]. If a state ρ achieves $R_\rho(|\alpha|^2)<R_{|n\rangle}$ for some $|\alpha|^2$, it possesses a capability to surpass the sensing with the Fock state $|n\rangle$. Therefore, the sequence $R_{|n\rangle}$ establishes a hierarchy of conditions for sensing classifying the states approaching Fock states. Figure 3 presents the metrological potential of realized states to pass these conditions. Specifically, realistic Fock states up to $n=10$ surpass the limit given by the vacuum state and the prepared state approaching the ideal Fock state $|8\rangle$ presents the capacity to exceed the Fock state $|5\rangle$. The realized state approaching $|10\rangle$ and all the higher prepared Fock states did not possess the metrological advantage against the ideal Fock state $|8\rangle$ due to noise mainly including the residual heating during the state preparation, see Supplemental Material, S2 [37].

For sensing of a small $|\alpha|^2$, the noise affects how far a prepared state is from the threshold given by the ideal Fock state $|n\rangle$. The advantage gets lost even for a very small noise in the high $|n\rangle$ limit. $R_\rho(|\alpha|^2)$ tends to saturate for displacement on the order of 10^{-2} and approaches the gain expectable for ideal Fock states. At the same time, employment of realistic states with high n in the limit of small displacements seems to be further favored due to effectively decreasing dependence of the offset in $R_\rho(|\alpha|^2)$ on n, when compared to ideal Fock states. This has been confirmed by a numerical simulation considering sensing with states resulting from thermalization of Fock states, see the Supplemental Material, S5 [37]. We note the visible deviation from this trend for the state approaching $|2\rangle$ caused by the analysis on the phonon distribution with residual $P_0\sim 1\%$, instead of the mixture of P_1 and P_3 expectable for the case of dominant spread through thermalization. However, these small populations are of a low statistical significance.

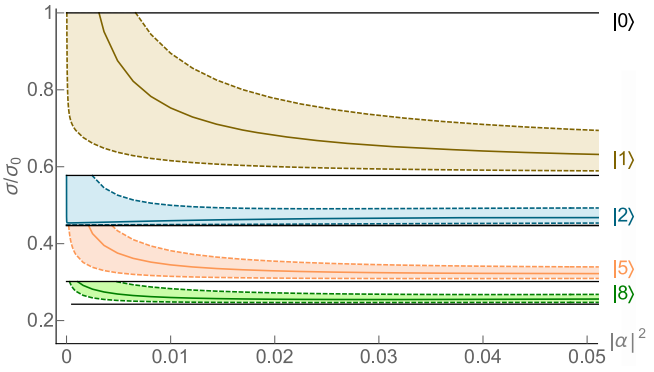

FIG. 3. Estimation of the metrological advantage of realized states for sensing of a small force. The horizontal axis quantifies the amplitude in the phase space that the force causes. The vertical axis shows the minimal standard deviation σ estimated by optimization of the Fisher information in Eq. (3) normalized to σ_0 resulting from sensing using a motional ground state. The black lines show σ/σ_0 for ideal Fock states. The brown, blue, orange, and green solid curves correspond to prepared states approaching the Fock states $|n\rangle=|1\rangle,|2\rangle,|5\rangle$, and $|8\rangle$, respectively. The colored regions show σ/σ_0 for states with the phonon-number distributions within experimental error bars.

Conclusions.—The presented demonstration of high-order genuine QNG states [24,26] provides the first feasible methodology for conclusive, hierarchical, and sensitive evaluation of mechanical Fock states. Simultaneously, it predicts development of methods for quantum-enhanced sensing of motional heating or coherent displacements on quantum mechanical oscillators [12]. Beyond these direct applications, it provides a fundamental milestone of experimental witnessing of intrinsic properties of highly nonclassical states applicable to a broad spectrum of applications of quantum-enhanced control and measurement of mechanical motion in optical frequency metrology [53,54], quantum error correction [15–17,34], tests of quantum thermodynamics [55,56], or gravitational wave detection [57]. Together with the recent demonstration of the viable preparation of states suggesting proximity to number states with up to $|n\rangle \sim 100$ in the same experimental platform [9], the presented approach will allow for optimization and comparison of these quantum states across different sensing scenarios with a clearly identifiable fundamental and application relevance [58,59]. The provided evaluation of provable quantum metrological advantage of the generated states for sensing of small displacements with motional probes close to ideal Fock states $|n\rangle$ for n up to 8 suggests the potential of the presented methodology as a tool for analysis of the preparation of large genuine QNG sensing states with energies and corresponding metrological stability gains substantially beyond current experimental capabilities of quantum sensing with atomic and mechanical oscillators [12,60,61].

L. L., L. S., and R. F. are grateful to the support from the Czech Science Foundation under the project GA21-13265X. L. P., T. P., A. L., and O. C., acknowledge the support by Grant No. GA19-14988S from the Czech Science Foundation and the project CZ.02.1.01/0.0/0.0/16_026/0008460 of MEYS CR. T. P., A. L. and O. C. acknowledge the project EMPIR 20FUN01 TSCAC, which received funding from the EMPIR programme co-financed by the participating States and from European Union's Horizon 2020 research and innovation programme. The research leading to these results has received funding from the H2020 European Programme under Grant Agreement No. 951737 NONGAUSS. L. P. acknowledges the internal project of Palacky University IGA-PrF-2021-006.

*slodicka@optics.upol.cz
†filip@optics.upol.cz

[1] D. Leibfried, D. M. Meekhof, B. E. King, C. Monroe, W. M. Itano, and D. J. Wineland, Phys. Rev. Lett. **77**, 4281 (1996).
[2] D. M. Meekhof, C. Monroe, B. E. King, W. M. Itano, and D. J. Wineland, Phys. Rev. Lett. **76**, 1796 (1996).
[3] C. Roos, T. Zeiger, H. Rohde, H. C. Nägerl, J. Eschner, D. Leibfried, F. Schmidt-Kaler, and R. Blatt, Phys. Rev. Lett. **83**, 4713 (1999).
[4] K. Toyoda, R. Hiji, A. Noguchi, and S. Urabe, Nature (London) **527**, 74 (2015).
[5] D. Kienzler, H.-Y. Lo, V. Negnevitsky, C. Flühmann, M. Marinelli, and J. P. Home, Phys. Rev. Lett. **119**, 033602 (2017).
[6] S. Ding, G. Maslennikov, R. Hablützel, H. Loh, and D. Matsukevich, Phys. Rev. Lett. **119**, 150404 (2017).
[7] J. Zhang, M. Um, D. Lv, J.-N. Zhang, L.-M. Duan, and K. Kim, Phys. Rev. Lett. **121**, 160502 (2018).
[8] C. Flühmann, T. L. Nguyen, M. Marinelli, V. Negnevitsky, K. Mehta, and J. P. Home, Nature (London) **566**, 513 (2019).
[9] K. C. McCormick, J. Keller, S. C. Burd, D. J. Wineland, A. C. Wilson, and D. Leibfried, Nature (London) **572**, 86 (2019).
[10] Y. Chu, P. Kharel, T. Yoon, L. Frunzio, P. T. Rakich, and R. J. Schoelkopf, Nature (London) **563**, 666 (2018).
[11] M. Gessner, A. Smerzi, and L. Pezzè, Phys. Rev. Lett. **122**, 090503 (2019).
[12] F. Wolf, C. Shi, J. C. Heip, M. Gessner, L. Pezzè, A. Smerzi, M. Schulte, K. Hammerer, and P. O. Schmidt, Nat. Commun. **10**, 2929 (2019).
[13] F. Hanamura, W. Asavanant, K. Fukui, S. Konno, and A. Furusawa, Phys. Rev. A **104**, 062601 (2021).
[14] K. Duivenvoorden, B. M. Terhal, and D. Weigand, Phys. Rev. A **95**, 012305 (2017).
[15] M. H. Michael, M. Silveri, R. T. Brierley, V. V. Albert, J. Salmilehto, L. Jiang, and S. M. Girvin, Phys. Rev. X **6**, 031006 (2016).
[16] L. Hu, Y. Ma, W. Cai, X. Mu, Y. Xu, W. Wang, Y. Wu, H. Wang, Y. Song, C.-L. Zou, S. M. Girvin, L. M. Duan, and L. Sun, Nat. Phys. **15**, 503 (2019).
[17] P. Campagne-Ibarcq, A. Eickbusch, S. Touzard, E. Zalys-Geller, N. E. Frattini, V. V. Sivak, P. Reinhold, S. Puri, S. Shankar, R. J. Schoelkopf, L. Frunzio, M. Mirrahimi, and M. H. Devoret, Nature (London) **584**, 368 (2020).
[18] A. Ghosh, W. Niedenzu, V. Mukherjee, and G. Kurizki, in *Thermodynamics in the Quantum Regime* (Springer, New York, 2018), pp. 37–66.
[19] G. Maslennikov, S. Ding, R. Hablützel, J. Gan, A. Roulet, S. Nimmrichter, J. Dai, V. Scarani, and D. Matsukevich, Nat. Commun. **10**, 202 (2019).
[20] M.-L. Cai, Z.-D. Liu, W.-D. Zhao, Y.-K. Wu, Q.-X. Mei, Y. Jiang, L. He, X. Zhang, Z.-C. Zhou, and L.-M. Duan, Nat. Commun. **12**, 1126 (2021).
[21] R. L. Hudson, Rep. Math. Phys. **6**, 249 (1974).
[22] M. Walschaers, PRX Quantum **2**, 030204 (2021).
[23] W. P. Schleich, *Quantum Optics in Phase Space* (John Wiley & Sons, New York, 2011).
[24] L. Lachman, I. Straka, J. Hloušek, M. Ježek, and R. Filip, Phys. Rev. Lett. **123**, 043601 (2019).
[25] U. Chabaud, D. Markham, and F. Grosshans, Phys. Rev. Lett. **124**, 063605 (2020).
[26] U. Chabaud, G. Roeland, M. Walschaers, F. Grosshans, V. Parigi, D. Markham, and N. Treps, PRX Quantum **2**, 020333 (2021).
[27] M. Brownnutt, M. Kumph, P. Rabl, and R. Blatt, Rev. Mod. Phys. **87**, 1419 (2015).
[28] M. Aspelmeyer, T. J. Kippenberg, and F. Marquardt, Rev. Mod. Phys. **86**, 1391 (2014).

[29] D. B. Higginbottom, L. Slodička, G. Araneda, L. Lachman, R. Filip, M. Hennrich, and R. Blatt, New J. Phys. **18**, 093038 (2016).
[30] I. Straka, L. Lachman, J. Hloušek, M. Miková, M. Mičuda, M. Ježek, and R. Filip, npj Quantum Inf. **4**, 4 (2018).
[31] I. Straka, A. Predojević, T. Huber, L. Lachman, L. Butschek, M. Miková, M. Mičuda, G. S. Solomon, G. Weihs, M. Ježek, and R. Filip, Phys. Rev. Lett. **113**, 223603 (2014).
[32] Y.-S. Ra, A. Dufour, M. Walschaers, C. Jacquard, T. Michel, C. Fabre, and N. Treps, Nat. Phys. **16**, 144 (2020).
[33] M. Walschaers, S. Sarkar, V. Parigi, and N. Treps, Phys. Rev. Lett. **121**, 220501 (2018).
[34] B. de Neeve, T.-L. Nguyen, T. Behrle, and J. P. Home, Nat. Phys. **18**, 296 (2022).
[35] R. Filip and L. Mišta, Jr., Phys. Rev. Lett. **106**, 200401 (2011).
[36] P. Zapletal, T. Darras, H. Le Jeannic, A. Cavaillès, G. Guccione, J. Laurat, and R. Filip, Optica **8**, 743 (2021).
[37] See Supplemental Material at http://link.aps.org/supplemental/10.1103/PhysRevLett.129.013602 for experimental details of preparation, measurement, and evaluation of phonon-number distributions of presented motional states, which includes Refs. [39–50].
[38] J. I. Cirac, R. Blatt, A. S. Parkins, and P. Zoller, Phys. Rev. Lett. **70**, 762 (1993).
[39] J. Eschner, B. Appasamy, and P. E. Toschek, Phys. Rev. Lett. **74**, 2435 (1995).
[40] J. I. Cirac, R. Blatt, and P. Zoller, Phys. Rev. A **49**, R3174 (1994).
[41] R. Blatt, J. I. Cirac, and P. Zoller, Phys. Rev. A **52**, 518 (1995).
[42] C. J. Myatt, B. E. King, Q. A. Turchette, C. A. Sackett, D. Kielpinski, W. M. Itano, C. Monroe, and D. J. Wineland, Nature (London) **403**, 269 (2000).
[43] L. Podhora, T. Pham, A. Lešundák, P. Obšil, M. Čížek, O. Číp, P. Marek, L. Slodička, and R. Filip, Adv. Quantum Technol. **3**, 2000012 (2020).
[44] M. Um, J. Zhang, D. Lv, Y. Lu, S. An, J.-N. Zhang, H. Nha, M. S. Kim, and K. Kim, Nat. Commun. **7**, 11410 (2016).
[45] D. Kienzler, H.-Y. Lo, B. Keitch, L. De Clercq, F. Leupold, F. Lindenfelser, M. Marinelli, V. Negnevitsky, and J. P. Home, Science **347**, 53 (2015).
[46] S. Schneider and G. J. Milburn, Phys. Rev. A **57**, 3748 (1998).
[47] M. Murao and P. L. Knight, Phys. Rev. A **58**, 663 (1998).
[48] R. Bonifacio, S. Olivares, P. Tombesi, and D. Vitali, Phys. Rev. A **61**, 053802 (2000).
[49] A. A. Budini, R. L. de Matos Filho, and N. Zagury, Phys. Rev. A **65**, 041402(R) (2002).
[50] H. C. J. Gan, G. Maslennikov, K.-W. Tseng, C. Nguyen, and D. Matsukevich, Phys. Rev. Lett. **124**, 170502 (2020).
[51] D. Leibfried, R. Blatt, C. Monroe, and D. Wineland, Rev. Mod. Phys. **75**, 281 (2003).
[52] J. Eschner, G. Morigi, F. Schmidt-Kaler, and R. Blatt, J. Opt. Soc. Am. B **20**, 1003 (2003).
[53] C. Hempel, B. Lanyon, P. Jurcevic, R. Gerritsma, R. Blatt, and C. Roos, Nat. Photonics **7**, 630 (2013).
[54] Y. Wan, F. Gebert, J. B. Wübbena, N. Scharnhorst, S. Amairi, I. D. Leroux, B. Hemmerling, N. Lörch, K. Hammerer, and P. O. Schmidt, Nat. Commun. **5**, 3096 (2014).
[55] M. F. Gely, M. Kounalakis, C. Dickel, J. Dalle, R. Vatré, B. Baker, M. D. Jenkins, and G. A. Steele, Science **363**, 1072 (2019).
[56] D. Gelbwaser-Klimovsky and G. Kurizki, Sci. Rep. **5**, 1 (2015).
[57] M. Tse *et al.*, Phys. Rev. Lett. **123**, 231107 (2019).
[58] W. Gorecki, S. Zhou, L. Jiang, and R. Demkowicz-Dobrzański, Quantum **4**, 288 (2020).
[59] A. Kubica and R. Demkowicz-Dobrzański, Phys. Rev. Lett. **126**, 150503 (2021).
[60] S. Schreppler, N. Spethmann, N. Brahms, T. Botter, M. Barrios, and D. M. Stamper-Kurn, Science **344**, 1486 (2014).
[61] E. Hebestreit, M. Frimmer, R. Reimann, and L. Novotny, Phys. Rev. Lett. **121**, 063602 (2018).